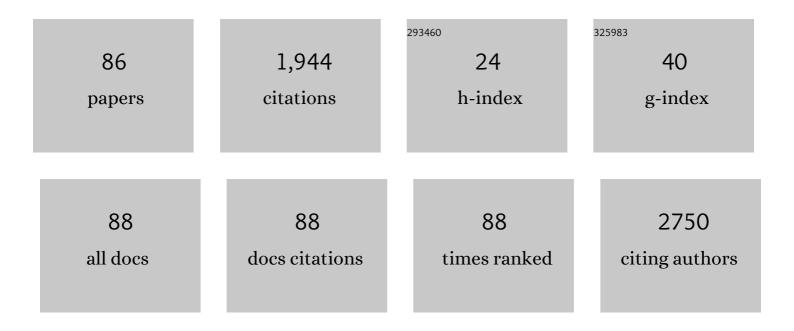
List of Publications by Year in descending order

Source: https://exaly.com/author-pdf/455568/publications.pdf Version: 2024-02-01



VIIAN MANC

#	Article	IF	CITATIONS
1	Dual roles of dissolved organic nitrogen in groundwater nitrogen cycling: Nitrate precursor and denitrification promoter. Science of the Total Environment, 2022, 811, 151375.	3.9	19
2	Investigation of the Oxidation Behavior of Cr20Mn17Fe18Ta23W22 and Microdefects Evolution Induced by Hydrogen Ions before and after Oxidation. Materials, 2022, 15, 1895.	1.3	1
3	Chemoselective Trimerization of Isocyanides: De Novo Synthesis of 2-Indole-Substituted Quinolines and Pyridines. Organic Letters, 2022, 24, 105-109.	2.4	12
4	Aging Affects Subcortical Pitch Information Encoding Differently in Humans With Different Language Backgrounds. Frontiers in Aging Neuroscience, 2022, 14, 816100.	1.7	0
5	Prevalence of Helicobacter pylori in Non-Cardia Gastric Cancer in China: A Systematic Review and Meta-Analysis. Frontiers in Oncology, 2022, 12, 850389.	1.3	8
6	β-1,6-Glucan From Pleurotus eryngii Modulates the Immunity and Gut Microbiota. Frontiers in Immunology, 2022, 13, 859923.	2.2	12
7	TMAO: how gut microbiota contributes to heart failure. Translational Research, 2021, 228, 109-125.	2.2	113
8	Noncontact Metal–Spiropyran–Metal Nanostructured Substrates with Ag and Au@SiO ₂ Nanoparticles Deposited in Nanohole Arrays for Surface-Enhanced Fluorescence and Trace Detection of Metal Ions. ACS Applied Nano Materials, 2021, 4, 3780-3789.	2.4	12
9	Toward a High-Performance Aqueous Zinc Ion Battery: Potassium Vanadate Nanobelts and Carbon Enhanced Zinc Foil. Nano Letters, 2021, 21, 2738-2744.	4.5	77
10	Similarity Evaluation on the Compound TCM Formulation "Huoling Shengji Granule―and Its Placebo by Intelligent Sensory Evaluation Technologies and the Human Sensory Evaluation Method Based on Critical Quality Attributes. Evidence-based Complementary and Alternative Medicine, 2021, 2021, 1-13.	0.5	1
11	Distribution Characteristics, Pollution Assessment, and Source Identification of Heavy Metals in Soils Around a Landfill-Farmland Multisource Hybrid District. Archives of Environmental Contamination and Toxicology, 2021, 81, 77-90.	2.1	11
12	GILT in tumor cells improves T cell-mediated anti-tumor immune surveillance. Immunology Letters, 2021, 234, 1-12.	1.1	5
13	Plasma Ceramides and Cardiovascular Events in Hypertensive Patients at High Cardiovascular Risk. American Journal of Hypertension, 2021, 34, 1209-1216.	1.0	9
14	Aldosterone dysregulation predicts the risk of mortality and rehospitalization in heart failure with a preserved ejection fraction. Science China Life Sciences, 2021, , 1.	2.3	5
15	Population Demographic History of a Rare and Endangered Tree Magnolia sprengeri Pamp. in East Asia Revealed by Molecular Data and Ecological Niche Analysis. Forests, 2021, 12, 931.	0.9	2
16	Characterization of the DNA molecular sequence of complete plastid genome of <i>Paeonia rockii</i> subsp. <i>taibaishanica</i> , an endemic species in China. Mitochondrial DNA Part B: Resources, 2021, 6, 2628-2629.	0.2	1
17	Association of IL1R1 Coding Variant With Plasma-Level Soluble ST2 and Risk of Aortic Dissection. Frontiers in Cardiovascular Medicine, 2021, 8, 710425.	1.1	5
18	Assessment and prediction of high speed railway bridge long-term deformation based on track geometry inspection big data. Mechanical Systems and Signal Processing, 2021, 158, 107749.	4.4	16

#	Article	IF	CITATIONS
19	Experimental and numerical investigations of asymmetric chord-reference system regarding track geometry measurement. Measurement: Journal of the International Measurement Confederation, 2021, 182, 109743.	2.5	7
20	Incidence and Survival of Aortic Dissection in Urban China: Results from the National Insurance Claims for Epidemiological Research (NICER) Study. The Lancet Regional Health - Western Pacific, 2021, 17, 100280.	1.3	11
21	Tailoring the Energy Band Structure and Interfacial Morphology of the ETL via Controllable Nanocluster Size Achieves High-Performance Planar Perovskite Solar Cells. ACS Applied Materials & Interfaces, 2021, 13, 48555-48568.	4.0	8
22	Vertical track irregularity analysis of high-speed railways on simply-supported beam bridges based on the virtual track inspection method. Proceedings of the Institution of Mechanical Engineers, Part F: Journal of Rail and Rapid Transit, 2021, 235, 328-338.	1.3	7
23	Quantitation and clinical evaluation of plasma aldosterone by ultra-performance liquid chromatography–mass spectrometry. Journal of Chromatography A, 2020, 1609, 460456.	1.8	9
24	Modeling and experimental verification of a fractional damping quad-stable energy harvesting system for use in wireless sensor networks. Energy, 2020, 190, 116301.	4.5	35
25	Using the geometric wheel-rail contact algorithms for fault detection in turnout areas based on the variable section characteristics of rails. Proceedings of the Institution of Mechanical Engineers, Part F: Journal of Rail and Rapid Transit, 2020, 234, 550-563.	1.3	4
26	Dynamic modeling and experimental investigation of self-powered sensor nodes for freight rail transport. Applied Energy, 2020, 257, 113969.	5.1	90
27	Reinforcement learning approach for optimal control of multiple electric locomotives in a heavy-haul freight train:A Double-Switch-Q-network architecture. Knowledge-Based Systems, 2020, 190, 105173.	4.0	26
28	High Curie Temperature Ferromagnetism and High Hole Mobility in Tensile Strained Mnâ€Đoped SiGe Thin Films. Advanced Functional Materials, 2020, 30, 2002513.	7.8	20
29	Subway rail transit monitoring by built-in sensor platform of smartphone. Frontiers of Information Technology and Electronic Engineering, 2020, 21, 1226-1238.	1.5	12
30	Electrophoretic Deposited Black Phosphorus on 3D Porous Current Collectors to Regulate Li Nucleation for Dendrite-Free Lithium Metal Anodes. ACS Applied Materials & Interfaces, 2020, 12, 51563-51572.	4.0	30
31	Beautiful chaotic patterns generated using simple untrained recurrent neural networks under harmonic excitation. Nonlinear Dynamics, 2020, 100, 3887-3905.	2.7	1
32	A new spinel high-entropy oxide (Mg _{0.2} Ti _{0.2} Zn _{0.2} Cu _{0.2} Fe _{0.2}) ₃ with fast reaction kinetics and excellent stability as an anode material for lithium ion batteries. RSC Advances, 2020, 10, 9736-9744.	O _{4< I.7}	/sub>
33	A Data-Fusion Approach for Speed Estimation and Location Calibration of a Metro Train Based on Low-Cost Sensors in Smartphones. IEEE Sensors Journal, 2019, 19, 10744-10752.	2.4	17
34	Tunable pseudocapacitive contribution by dimension control in nanocrystalline-constructed (Mg _{0.2} Co _{0.2} Ni _{0.2} Cu _{0.2} Zn _{0.2})O solid solutions to achieve superior lithium-storage properties. RSC Advances, 2019, 9, 28908-28915.	1.7	36
35	Theoretical and Experimental Studies of the Antislip Capacity between Cable and Saddle Equipped with Horizontal Friction Plates. Journal of Bridge Engineering, 2019, 24, .	1.4	7
36	Association of Soluble ST2 Serum Levels With Outcomes in Pediatric Dilated Cardiomyopathy. Canadian Journal of Cardiology, 2019, 35, 727-735.	0.8	14

#	Article	IF	CITATIONS
37	Excellent Electrochemical Performances of Intrinsic Polyaniline Nanofibers Fabricated by Electrochemical Deposition. Journal Wuhan University of Technology, Materials Science Edition, 2019, 34, 216-222.	0.4	11
38	Multipoint chord reference system for track irregularity: Part I – Theory and methodology. Measurement: Journal of the International Measurement Confederation, 2019, 138, 240-255.	2.5	15
39	Multipoint chord reference system for track irregularity: Part II – Numerical analysis. Measurement: Journal of the International Measurement Confederation, 2019, 138, 194-205.	2.5	9
40	Stress corrosion cracking behavior of 310S stainless steel in supercritical water at different temperature. Materials and Corrosion - Werkstoffe Und Korrosion, 2019, 70, 868-876.	0.8	1
41	Global Tudor‣N transgenic mice are protected from obesityâ€induced hepatic steatosis and insulin resistance. FASEB Journal, 2019, 33, 3731-3745.	0.2	4
42	Study on an elastic lever system for electromagnetic energy harvesting from rail vibration. Journal of Vibroengineering, 2019, 21, 384-395.	0.5	6
43	Stress corrosion cracking behavior of 310S in supercritical water with different oxygen concentrations. Nuclear Science and Techniques/Hewuli, 2018, 29, 1.	1.3	1
44	Experimental investigation of non-linear multi-stable electromagnetic-induction energy harvesting mechanism by magnetic levitation oscillation. Applied Energy, 2018, 220, 856-875.	5.1	132
45	The Complement C3a <i>–</i> C3aR Axis Promotes Development of Thoracic Aortic Dissection via Regulation of MMP2 Expression. Journal of Immunology, 2018, 200, 1829-1838.	0.4	36
46	Synthesis of manganese-based complex as cathode material for aqueous rechargeable batteries. RSC Advances, 2018, 8, 15703-15708.	1.7	14
47	Error theory of chord-based measurement system regarding track geometry and improvement by high frequency sampling. Measurement: Journal of the International Measurement Confederation, 2018, 115, 204-216.	2.5	16
48	Magnitude of Soluble ST2 as a Novel Biomarker for Acute Aortic Dissection. Circulation, 2018, 137, 259-269.	1.6	80
49	Experimental Study on Rockfall Impact Force Applied to Frame Shed Tunnels. Journal of Highway and Transportation Research and Development (English Edition), 2018, 12, 59-66.	0.2	4
50	Traffic Command Gesture Recognition for Virtual Urban Scenes Based on a Spatiotemporal Convolution Neural Network. ISPRS International Journal of Geo-Information, 2018, 7, 37.	1.4	26
51	The increasing variability of tropical cyclone lifetime maximum intensity. Scientific Reports, 2018, 8, 16641.	1.6	15
52	Response by Wang et al to Letter Regarding Article, "Magnitude of Soluble ST2 as a Novel Biomarker for Acute Aortic Dissection― Circulation, 2018, 138, 1281-1282.	1.6	1
53	Both Gfrα1a and Gfrα1b Are Involved in the Self-Renewal and Maintenance of Spermatogonial Stem Cells in Medaka. Stem Cells and Development, 2018, 27, 1658-1670.	1.1	10
54	A Bayesian modeling approach for phosphorus load apportionment in a reservoir with high water transfer disturbance. Environmental Science and Pollution Research, 2018, 25, 32395-32408.	2.7	7

#	Article	IF	CITATIONS
55	A light-driven molecular machine based on stiff stilbene. Chemical Communications, 2018, 54, 7991-7994.	2.2	47
56	Experimental and Numerical Study on Buckling Behavior of a Rigidly Stiffened Plate with Tee Ribs. International Journal of Steel Structures, 2018, 18, 582-595.	0.6	3
57	Position synchronization for track geometry inspection data via big-data fusion and incremental learning. Transportation Research Part C: Emerging Technologies, 2018, 93, 544-565.	3.9	28
58	Development and validation of an LC–MS/MS method for the simultaneous quantification of seven constituents in rat plasma and application in a pharmacokinetic study of the Zaoren Anshen prescription. Biomedical Chromatography, 2018, 32, e4055.	0.8	7
59	Asymmetric interaction of point defects and heterophase interfaces in ZrN/TaN multilayered nanofilms. Scientific Reports, 2017, 7, 40044.	1.6	9
60	Synthesis and evaluation of novel ascorbyl cinnamates as potential anti-oxidant and antimicrobial agents. Research on Chemical Intermediates, 2017, 43, 5901-5916.	1.3	2
61	ER stress dependent microparticles derived from smooth muscle cells promote endothelial dysfunction during thoracic aortic aneurysm and dissection. Clinical Science, 2017, 131, 1287-1299.	1.8	66
62	Metabolomics through the lens of precision cardiovascular medicine. Journal of Genetics and Genomics, 2017, 44, 127-138.	1.7	21
63	The stabilization of the rocksalt structured tantalum nitride. Journal of Applied Physics, 2017, 122, .	1.1	9
64	A new self-tuning fuzzy controller for vibration of a flexible structure subjected to multi-frequency excitations. Proceedings of the Institution of Mechanical Engineers Part I: Journal of Systems and Control Engineering, 2017, 231, 614-625.	0.7	2
65	Realistic image composite with best-buddy prior of natural image patches. , 2017, , .		0
66	A Meta-Analysis for Association of Maternal Smoking with Childhood Refractive Error and Amblyopia. Journal of Ophthalmology, 2016, 2016, 1-7.	0.6	8
67	Rheological Properties of Municipal Sewage Sludge: Dependency on Solid Concentration and Temperature. Procedia Environmental Sciences, 2016, 31, 113-121.	1.3	39
68	Reporter-Embedded SERS Tags from Gold Nanorod Seeds: Selective Immobilization of Reporter Molecules at the Tip of Nanorods. ACS Applied Materials & Interfaces, 2016, 8, 28105-28115.	4.0	50
69	Photoresponse properties based on CdS nanoparticles deposited on multi-walled carbon nanotubes. RSC Advances, 2016, 6, 78053-78058.	1.7	8
70	Senkyunolide I attenuates oxygen-glucose deprivation/reoxygenation-induced inflammation in microglial cells. Brain Research, 2016, 1649, 123-131.	1.1	39
71	Highly sensitive and well reproducible Surface-enhanced Raman spectroscopy from silver triangular platelets. Talanta, 2016, 161, 599-605.	2.9	14
72	MDG-1, an Ophiopogon polysaccharide, alleviates hyperlipidemia in mice based on metabolic profile of bile acids. Carbohydrate Polymers, 2016, 150, 74-81.	5.1	37

YUAN WANG

#	Article	IF	CITATIONS
73	T-shaped monopyridazinotetrathiafulvalene-amino acid diad based chiral organogels with aggregation-induced fluorescence emission. Soft Matter, 2016, 12, 6373-6384.	1.2	12
74	Senkyunolide I protects rat brain against focal cerebral ischemia–reperfusion injury by up-regulating p-Erk1/2, Nrf2/HO-1 and inhibiting caspase 3. Brain Research, 2015, 1605, 39-48.	1.1	73
75	Ultraviolet membrane bioreactor for enhancing the removal of organic matter in micro-polluted water. Desalination and Water Treatment, 2015, 56, 2335-2343.	1.0	0
76	MDG-1, an Ophiopogon polysaccharide, regulate gut microbiota in high-fat diet-induced obese C57BL/6 mice. International Journal of Biological Macromolecules, 2015, 81, 576-583.	3.6	75
77	Electrochemical performance of patterned LiFePO4 nano-electrode with a pristine amorphous layer. Applied Physics Letters, 2014, 104, .	1.5	8
78	Immobilization of heparin/poly-l-lysine nanoparticles on dopamine-coated surface to create a heparin density gradient for selective direction of platelet and vascular cells behavior. Acta Biomaterialia, 2014, 10, 1940-1954.	4.1	126
79	UPLC-TOF/MS based urinary metabonomic studies reveal mild prevention effects of MDG-1 on metabolic disorders in diet-induced obese mice. Analytical Methods, 2014, 6, 4171.	1.3	4
80	MDG-1, a polysaccharide from Ophiopogon japonicus, prevents high fat diet-induced obesity and increases energy expenditure in mice. Carbohydrate Polymers, 2014, 114, 183-189.	5.1	50
81	Thermal distribution analysis of multi-core photonic crystal fiber laser. Optoelectronics Letters, 2012, 8, 13-16.	0.4	5
82	Design, synthesis and bioactivity of ethyl 2-((1-methyl-2, 3-dioxoindolin-5-yl) methoxy) acetate. , 2011, , .		0
83	Dichlorido[N′-(3,5-dichloro-2-hydroxybenzylidene)pyridine-4-carbohydrazide-κN](1,10-phenanthroline-κ2N,Ná methanol monosolvate. Acta Crystallographica Section E: Structure Reports Online, 2009, 65, m1594-m1594.	′)cobalt 0.2	(II) 1
84	(3,5-Dichlorosalicylaldehyde thiosemicarbazonato-κ3S,N1,O)(N,N′-dimethylformamide-κO)copper(II) dimethylformamide solvate. Acta Crystallographica Section E: Structure Reports Online, 2008, 64, m633-m634.	0.2	1
85	Calcium-Mediated Mitochondrial Permeability Transition Involved in Hydrogen Peroxide-Induced Apoptosis in Tobacco Protoplasts. Journal of Integrative Plant Biology, 2006, 48, 433-439.	4.1	16
86	Salt stress-induced programmed cell death via Ca2+-mediated mitochondrial permeability transition in tobacco protoplasts. Plant Crowth Pergulation, 2005, 45, 243-250	1.8	51

tobacco protoplasts. Plant Growth Regulation, 2005, 45, 243-250.